



## OPEN ACCESS

## EDITED BY

Ronaldo Thomatieli-Santos,  
Federal University of São Paulo, Brazil

## REVIEWED BY

Niroj Kumar Sethy,  
Defence Institute of Physiology and Allied  
Sciences (DRDO), India  
Juliana Schlaad,  
Santa Casa of Sao Paulo, Brazil

## \*CORRESPONDENCE

Fengming Luo,  
✉ fengmingluo@outlook.com

## †PRESENT ADDRESS

Ling Chen,  
Center for High Altitude Medicine, West China  
Hospital, Sichuan University, Chengdu, China

†These authors have contributed equally  
to this work

RECEIVED 09 December 2025

REVISED 18 January 2026

ACCEPTED 23 January 2026

PUBLISHED 18 February 2026

## CITATION

Chen L, He X, Wang H, Hu S, Zhao H, Ni G,  
Yan H, Chen L, Deng C and Luo F (2026)  
Physiological and molecular dynamic changes  
during 23-day high-altitude exposure reveal  
novel biomarkers for acclimatization.  
*Front. Physiol.* 17:1763837.  
doi: 10.3389/fphys.2026.1763837

## COPYRIGHT

© 2026 Chen, He, Wang, Hu, Zhao, Ni, Yan,  
Chen, Deng and Luo. This is an open-access  
article distributed under the terms of the  
[Creative Commons Attribution License \(CC  
BY\)](https://creativecommons.org/licenses/by/4.0/). The use, distribution or reproduction in  
other forums is permitted, provided the  
original author(s) and the copyright owner(s)  
are credited and that the original publication  
in this journal is cited, in accordance with  
accepted academic practice. No use,  
distribution or reproduction is permitted  
which does not comply with these terms.

# Physiological and molecular dynamic changes during 23-day high-altitude exposure reveal novel biomarkers for acclimatization

Ling Chen<sup>1,2†</sup>, Xuefei He<sup>1,3†</sup>, Hao Wang<sup>4†</sup>, Sihu Hu<sup>2</sup>,  
Haitong Zhao<sup>1,5</sup>, Guohua Ni<sup>1,5</sup>, Hui Yan<sup>5</sup>, Lei Chen<sup>1,4</sup>,  
Cheng Deng<sup>1,3,6</sup> and Fengming Luo<sup>1,2,4\*</sup>

<sup>1</sup>Department of High Altitude Medicine, High Altitude Medicine Key Laboratory of Sichuan Province, Center for High Altitude Medicine, West China Hospital, Sichuan University, Chengdu, Sichuan, China,

<sup>2</sup>Laboratory of Pulmonary Immunology and Inflammation, Frontiers Science Center for Disease-related Molecular Network, West China Hospital, Sichuan University, Chengdu, Sichuan, China, <sup>3</sup>Institute of High Altitude Medicine, National Clinical Research Center for Geriatrics, West China Hospital, Sichuan University, Chengdu, Sichuan, China, <sup>4</sup>Department of Respiratory and Critical Care Medicine, West China Hospital, Sichuan University, Chengdu, Sichuan, China, <sup>5</sup>Emergency Management Office, West China Hospital, Sichuan University, Chengdu, China, <sup>6</sup>Center for High Altitude Medicine, Xining, Qinghai, China

**Introduction:** Health conditions associated with rapid ascent to high altitudes remain prevalent and pose an ongoing challenge. While acute mountain sickness (AMS) typically occurs within the first few days after ascent, the physiological and molecular acclimatization processes during prolonged high-altitude exposure beyond the initial acute phase remain incompletely understood.

**Methods:** This cross-sectional study investigated physiological and transcriptomic dynamics during prolonged high-altitude exposure over a 23 day period at 4,104 m in 113 Chinese Han individuals. Linear regression analysis, time series analysis, enrichment analysis, and protein-protein interaction analysis were applied to reveal the physiological and molecular dynamic changes.

**Results:** Four physiological parameters (saturation of peripheral oxygen [SpO<sub>2</sub>], hemoglobin, hematocrit, and standard deviation of red blood cell distribution width [RDW-SD]) exhibit a significant positive linear trend with the duration of acclimatization at high altitude (DAHA). Notably, two distinct gene expression patterns (GEPs) following DAHA were characterized for the first time: a decreasing expression pattern (Pattern 1) and a “mountain-shaped” expression pattern—upregulated in the first week and then downregulated (Pattern 2). In comparing individuals who experienced or were experiencing acute mountain sickness (eAMS+, n = 56) with those who did not (eAMS-, n = 57), RNA-seq performed in a subset of 48 participants (eAMS+, n = 35; eAMS-, n = 13) identified 583 upregulated and 104 downregulated genes in the eAMS+ group. Among these, 398 upregulated genes and 10 enriched pathways were found to overlap with Pattern 2. By integrating baseline data from the GSE75665 database, five hub differentially expressed genes (DEGs)—*BCL2L1*, *DCAF12*, *CDC34*, *PINK1*, and *UBB*—were identified. These genes not only predict AMS susceptibility but also associated with molecular responses to prolonged high-altitude exposure. In particular, *CDC34* and *UBB* are novel genes not previously mentioned.

**Conclusion:** This study provides critical insights into key physiological trends and molecular expression dynamics associated with prolonged exposure to high-altitude environments.

#### KEYWORDS

acclimatization process, acute mountain sickness (AMS), gene expression pattern (GEP), high-altitude exposure, temporal transcriptome analysis

## 1 Introduction

Rapid ascent to high altitude induces a series of hypoxia-driven pathophysiological responses that collectively aim to maintain tissue oxygen homeostasis. These responses involve oxygen content restoration and compensatory oxygen delivery mechanisms (Julian, 2007; Zhang et al., 2014; Calbet et al., 2002), as reflected in the hypoxic ventilatory response (Weil et al., 1970; Swenson et al., 1985), hypoxic pulmonary vasoconstriction (Dehnert et al., 2005; Swenson, 2013), and changes in cerebral blood flow (Lucas et al., 2011). Together, these processes constitute the physiological basis of human acclimatization to hypobaric hypoxia following ascent to high altitude, representing an environmentally driven and non-genetic state distinct from long-term genetic adaptation (Cheng et al., 2025).

Despite the existence of shared acclimated mechanisms, individual responses to hypoxia vary substantially. Such inter-individual heterogeneity is closely linked to susceptibility to acute mountain sickness (AMS), a common high-altitude that typically manifests within the first few days after ascent (Sikri and Bhattachar, 2017).

AMS remains high prevalent, particularly among the lowland Han population (Buroker et al., 2012), and poses considerable economic burdens, safety issues (Hultgren, 1979), and even life-threatening situations (Luks et al., 2017). Previous researches have shown that physiological, cellular, and molecular responses occurring shortly after altitude exposure are crucial to AMS onset and development (Basnyat and Starling, 2015). However, the biological mechanisms underlying differential AMS susceptibility among individuals exposed to similar hypoxic environments remain incompletely clear.

Advances in genomic and transcriptomic profiling have enabled the identification of genetic variants and molecular pathways associated with hypoxia acclimatization and AMS susceptibility (Sharma et al., 2022). Several transcriptomic studies have specially investigated AMS, reporting differential expression of genes involved in inflammation, immune regulation, oxidative stress, and energy metabolism during the early phase of high-altitude exposure. Existing studies have implicated pathways related to inflammatory and immune response (Pham et al., 2022), cellular metabolism (Chen et al., 2012), and erythropoiesis (Pham et al., 2024) in hypoxia responses and altitude-related physiological adjustment (Subudhi et al., 2014). Nevertheless, most prior transcriptomic investigations have focused on early or acute exposure periods, and the relationships among gene expression patterns, biological pathways, and physiological phenotypes during prolonged high-altitude exposure beyond the initial acute phase remain poorly characterized. In particular, it is unclear whether distinct temporal gene expression patterns emerge at the population

level and how such patterns relate to AMS susceptibility and physiological adjustment.

To address these gaps, we aimed to gain a more comprehensive understanding of the acclimatization process by analyzing dynamic physiological and molecular changes following high-altitude exposure. Physical examination, AMS symptoms assessment and RNA sequencing (Liew et al., 2006; Kohane and Valtchinov, 2012) were performed. A time-point-based analytical framework was applied across individuals with varying durations of high-altitude exposure to evaluate exposure-associated dynamic under hypobaric hypoxia. Gene clustering, enriched pathway analysis, and network analysis were used to identify gene expression patterns (GEPs) and hub genes for AMS susceptibility and acclimatization. In total, 113 Chinese Han individuals exposure to high altitude for up to 23 days were enrolled. Four physical parameters exhibited a positive linear relationship with the duration of acclimatization at high altitude (DAHA). Two distinct GEPs and their associated biological pathways were identified. In addition, five hub genes with two novel genes were found as potential key biomarkers for AMS susceptibility and the acclimatization process.

## 2 Results

### 2.1 Demographic characteristics

A total of 113 Chinese Han individuals (104 males, 9 females), aged between 18 and 63, were enrolled in this cross-sectional study. Among them, 56 had experienced or were experiencing acute mountain sickness (eAMS+), while 57 did not. DAHA ranged from 1 to 23 days (Supplementary Figure S1; Table 1). Participants were categorized into four groups based on DAHA: T1 ( $\leq 3$  days,  $n = 22$ ), T2 (4–7 days,  $n = 18$ ), T3 (8–14 days,  $n = 29$ ), and T4 (15–23 days,  $n = 44$ ). The Kruskal–Wallis test revealed no significant demographic differences (sex, age, BMI, eAMS) among the four DAHA groups (Table 2). Chi-square test or t-test suggested no demographic differences among eAMS + group and eAMS- group (Table 3).

### 2.2 Correlations between physiological parameters and the DAHA

We analyzed 44 physiological parameters (Supplementary Table S1) to define acclimatization traits. After excluding sample S187 for excessive missing data (17 out of 44 items, 38.64%), principal component analysis (PCA) was performed on 112 individuals. Four additional outliers (S381, S472, S15, S13) out of 95% confidence intervals were removed (Figures 1a,b). Multiple linear regression

TABLE 1 Distribution of population characteristics.

Characteristics	Min	1st Qu	Median	Mean	3rd Qu	Max
Age(y/o)	18	29.00	37.00	38.39	47.00	63.00
BMI(kg/m <sup>2</sup> )	16.60	21.70	23.40	23.51	25.10	33.80
eAMS score	0	0	0	1.91	4.00	8.00
DAHA(days)	1.00	5.00	13.00	10.96	15.00	23.00

Qu, quartile; BMI, body mass index; eAMS, experienced or experiencing acute mountain sickness; DAHA, days of acclimatization at high altitude.

TABLE 2 Bias results of population characteristics among the four DAHA groups.

Characteristics	$\chi^2$	df	p value
Gender	2.63	1	0.1051
Age(y/o)	36.98	35	0.3778
BMI(kg/m <sup>2</sup> )	60.17	63	0.5778
eAMS(+/-)	6.93	5	0.2262

$\chi^2$ , chi-square, df, degrees of freedom.

model (adjusted for age, sex, and BMI) identified four parameters exhibiting a significant linear relationship with DAHA after adjusting for multiple comparisons via the Benjamini–Hochberg method (FDR < 0.05). These parameters included saturation of peripheral oxygen (SpO<sub>2</sub>,  $r = 0.331$ ), hemoglobin (HGB,  $r = 0.602$ ), hematocrit (HCT,  $r = 0.553$ ), and the standard deviation of red blood cell distribution width (RDW-SD,  $r = 0.46$ ) (Figures 1c–f; Supplementary Table S2). However, only RDW-SD remained significant in the subsequent Kruskal–Wallis test (FDR = 0.0066, Supplementary Table S3).

### 2.3 Time series analysis reveals the expression trends of genes in the DAHA groups

To explore the relationship between GEPs and DAHA, we performed transcriptomics on a subset of 48 individuals with complete RNA sequencing data (including 35 eAMS+ and 13 eAMS- participants). Their DAHA ranged from 2 to 19 days and were divided into T1 ( $\leq 3$  days,  $n = 4$ ), T2 (4–7 days,  $n = 11$ ), T3 (8–14 days,  $n = 17$ ), and T4 (15–19 days,  $n = 16$ ) (Supplementary Figures S2a,b). Using Fuzzy C-Means Clustering (FCM) clustering algorithm, genes were grouped into 12 clusters with distinct temporal dynamics. Among these, Cluster 4 (C4,  $n = 1,389$ ) and Cluster 9 (C9,  $n = 1,469$ ) showed consistently increasing and decreasing gene expression over time, respectively (Figure 2a; Supplementary Figure S2c). C4 was enriched in adaptive immune response, nonsense-mediated decay independent of the exon junction complex, steroid biosynthesis, and the regulation of protein transport. And C9 was linked to the regulation of the response to biotic stimuli, the innate immune

response, neutrophil degradation, interferon gamma signaling, the regulation of immune effector processes, and other immune or inflammatory pathways (Supplementary Figures S2d,e).

Moreover, differentially expressed gene (DEG) analysis across DAHA groups revealed distinct gene changes in each period: P1 (T2 vs. T1, 681 up, 169 down), P2 (T3 vs. T2, 205 up, 108 down), and P3 (T4 vs. T3, 217 up, 486 down) ( $p < 0.05$ ,  $|\log_{2}FC| > 0.3785$ ) (Figure 2b). Hallmark Gene Set Enrichment Analysis (HGSEA) revealed that heme metabolism was upregulated in P1 then downregulated in P2 and P3, aligned with, the “acute increase followed by decrease” expression trend of Cluster 8 (C8). Interferon alpha/gamma response were not different in P1 but significantly downregulated in P2 and P3 ( $p < 0.05$ ,  $q < 0.25$ , and  $|\text{Normalized Enrichment Score (NES)}| > 1$ ) (Figure 2c). C8 was specially enriched in heme metabolism ( $p = 1e-10$ ,  $q = 4e-9$ ,  $\text{NES} = 2.13$ ), while the interferon alpha/gamma response was enriched in C9. In contrast, no significant HGSEA results were identified for C4 (Supplementary Table S4). Based on the expression trends and enrichment results, the functional characteristics of C4, C8, and C9 were further compared.

### 2.4 Weighted gene coexpression network analysis (WGCNA) reveals the relationships between gene modules and phenotypes

We performed WGCNA on the transcriptomic data to investigate gene modules associated with DAHA. After excluding 3 outlier samples identified by hierarchical clustering identified, a soft threshold power of 6 was selected for network construction (Supplementary Figures S3a,b). The gene set was divided into modules using an adjacency matrix, which quantifies the pairwise correlations with genes. To ensure robust module definitions, modules with over 75% similarity were merged, resulting in 26 distinct modules (Supplementary Figure S3c). Among these, the darkorange module (DO) presented a significant negative correlation with DAHA ( $r = -0.3$ ,  $p = 0.048$ ). Conversely, the darkmagenta module (DM) was positively correlated ( $r = 0.39$ ,  $p = 0.0086$ ). Significant correlations with eAMS were identified: positive for the blue module (BL;  $r = 0.35$ ,  $p = 0.019$ ) and negative for DO ( $r = -0.34$ ,  $p = 0.021$ ) (Supplementary Figure S3d).

Enrichment analysis showed that DO-associated genes ( $n = 114$ ) were linked to several key immune processes such as the antiviral defense response and interferon response, sharing similar expression trends and functions with C9. In contrast, the DM

TABLE 3 Bias results of population characteristics among eAMS+ and eAMS- groups.

Characteristics	Level	eAMS- (n = 57)	eAMS+ (n = 56)	p value
Gender	Female	3 (5.3)	6 (10.7)	0.47
	Male	54 (94.7)	50 (89.3)	
Age (y/o)		39.65 (11.47)	37.11 (10.68)	0.226
BMI (kg/m <sup>2</sup> )		23.83 (3.05)	23.19 (3.16)	0.277
DAHA		11.75 (5.44)	10.16 (6.34)	0.154

BMI, body mass index; DAHA, days of acclimatization at high altitude.

(n = 37) were involved in memory and ion transport, while BL (n = 1911) was significantly enriched in protein catabolic, cellular stress responses, metabolic processes, and autophagy regulation (Supplementary Figure S4).

## 2.5 Gene expression patterns and hub genes identified over time

Using integrated analysis of time series and WGCNA, we identified 18 high-confidence genes shared between the DM module and C4, both positively associated with the DAHA (Figure 3a). These genes were associated primarily with the negative regulation of hydrolase activity (3 genes), inorganic ion transmembrane transport (4 genes), and intracellular chemical homeostasis (3 genes) (Supplementary Figure S5a). Although 15 of these genes were found in the STRING database, protein-protein interaction (PPI) network analysis revealed no significant associations among them (Supplementary Figure S5b).

The gene set with a decreasing expression trend with DAHA, the DO module and C9 shared 90 immunity-related genes involved in antiviral defense, interferon responses, and tuberculosis immunity. To pinpoint key genes, we imported the PPI results into Cytoscape. The top 5% (n = 5) of genes with the highest degree centrality were selected as hub genes: *STAT1*, *OAS1*, *OAS2*, *RSAD2*, and *IFI44*. Considering the consistent expression trend and functional profile of this intersection gene set, we designated it as Pattern 1 (Figures 3a,b,d).

The BL module shared 85 genes with C4, enriched in pathways including the Nop56p-associated pre-rRNA complex (4 genes), insulin receptor signaling pathway (3 genes), cholesterol metabolic process (3 genes), positive regulation of the MAPK cascade (5 genes) and positive regulation of translation (3 genes) (Supplementary Figure S5c). It also shared 86 genes with C9, which were linked to organic acid catabolic processes (4 genes), proteinogenic amino acid metabolic processes (3 genes), and herpes simplex virus 1 infection (3 genes) (Supplementary Figure S5d).

For C8, the BL module presented the highest gene overlap. These genes were enriched in processes like protein ubiquitination, erythrocyte differentiation, autophagy, and mitophagy. The top 20 hub genes were identified via PPI network analysis. These genes comprised *UBA52*, *UBB*, *FECH*, *SNCA*, *SLC4A1*, *GATA1*, *RBX1*, *ALAS2*, *SKP1*, *EPB42*, *GYPB*, *KLF1*, *PSMD4*, *ANK1*, *CDC34*,

*PINK1*, *BCL2L1*, *DMTN*, *DCAF12*, and *GYPB*. The “mountain-shaped” expression pattern of these 818 genes was defined as Pattern 2 (Figures 3a,c,e).

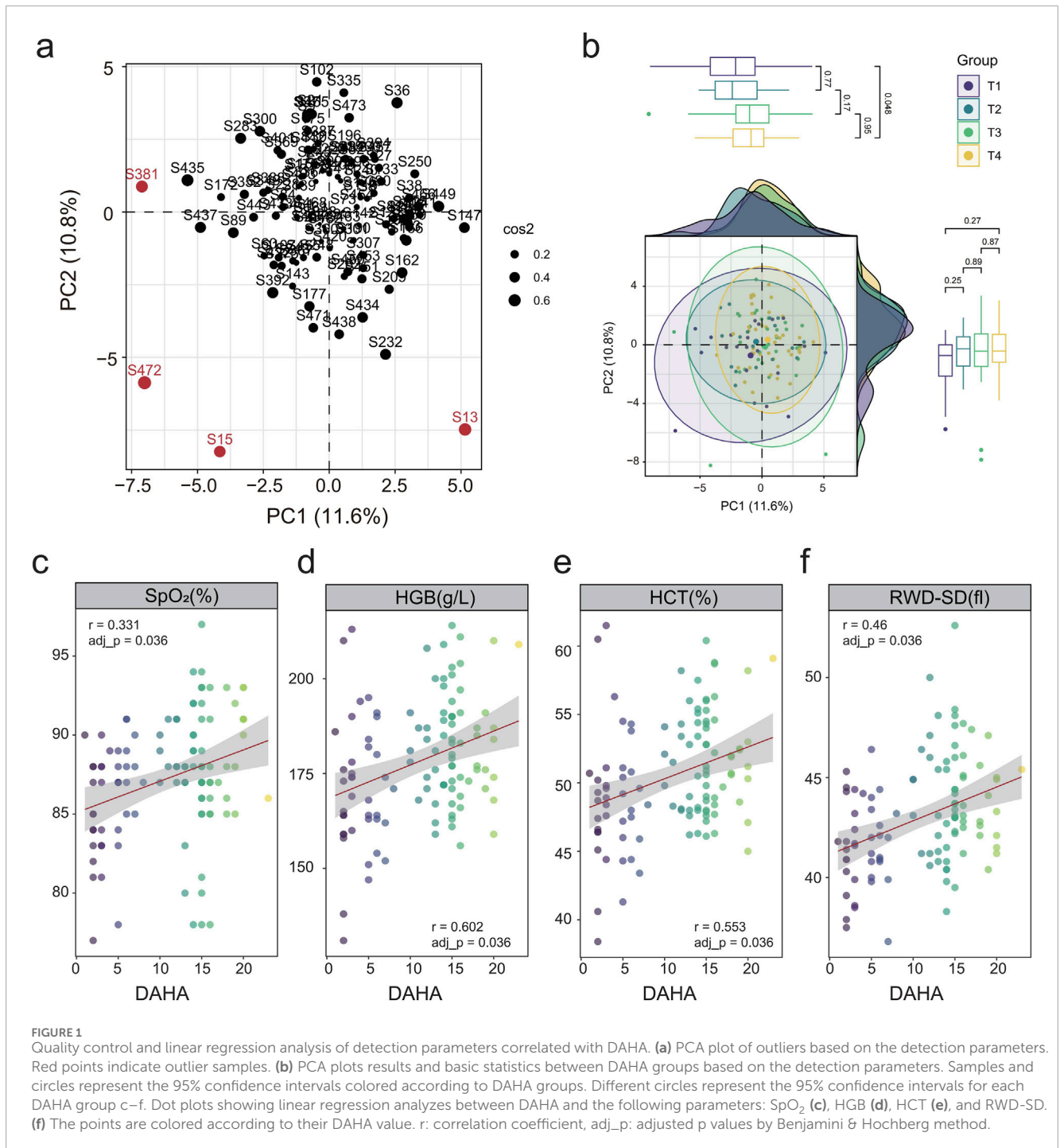
## 2.6 Hub genes highly correlated with the physiological phenotype

Furthermore, we investigated the correlations between the hub genes and the 44 physiological parameters mentioned above. Hub genes in Pattern 1 were negatively correlated with plateletcrit (PCT) and platelets (PLTs). Key correlations included *STAT1* negative with the percentage of monocytes (MONOP) and mean corpuscular hemoglobin concentration (MCHC). *OAS1* positive with creatinine (CREA) and aspartate aminotransferase (AST), *OAS2* positive with HCT and HGB, and *IFI44* weakly positive with the white blood cell (WBC) count.

In Pattern 2, nearly all hub genes correlated negatively with immune cells like WBC, monocyte count (MONO), MONOP, neutrophil count (NEUT), lymphocyte count (LYMPH) and hematological parameters like HCT, red blood cell count (RBC) and HGB, but were positively correlated with CREA. *UBA52*, the hub gene with the highest degree in Pattern 2, exhibited positive correlation with the percentage of eosinophils (EOP), aspartate aminotransferase/alanine aminotransferase (ASL/ALT), and direct bilirubin (DBIL), and negative correlation with the platelet distribution width (PDW), low-density lipoprotein cholesterol (LDLC), and total cholesterol (TC). Notably, *PSMD4* presented the strongest positive correlation with CREA among all Pattern 2 hub genes (Supplementary Figure S6).

## 2.7 Differences between the eAMS+ and eAMS- groups in pattern 1 and pattern 2

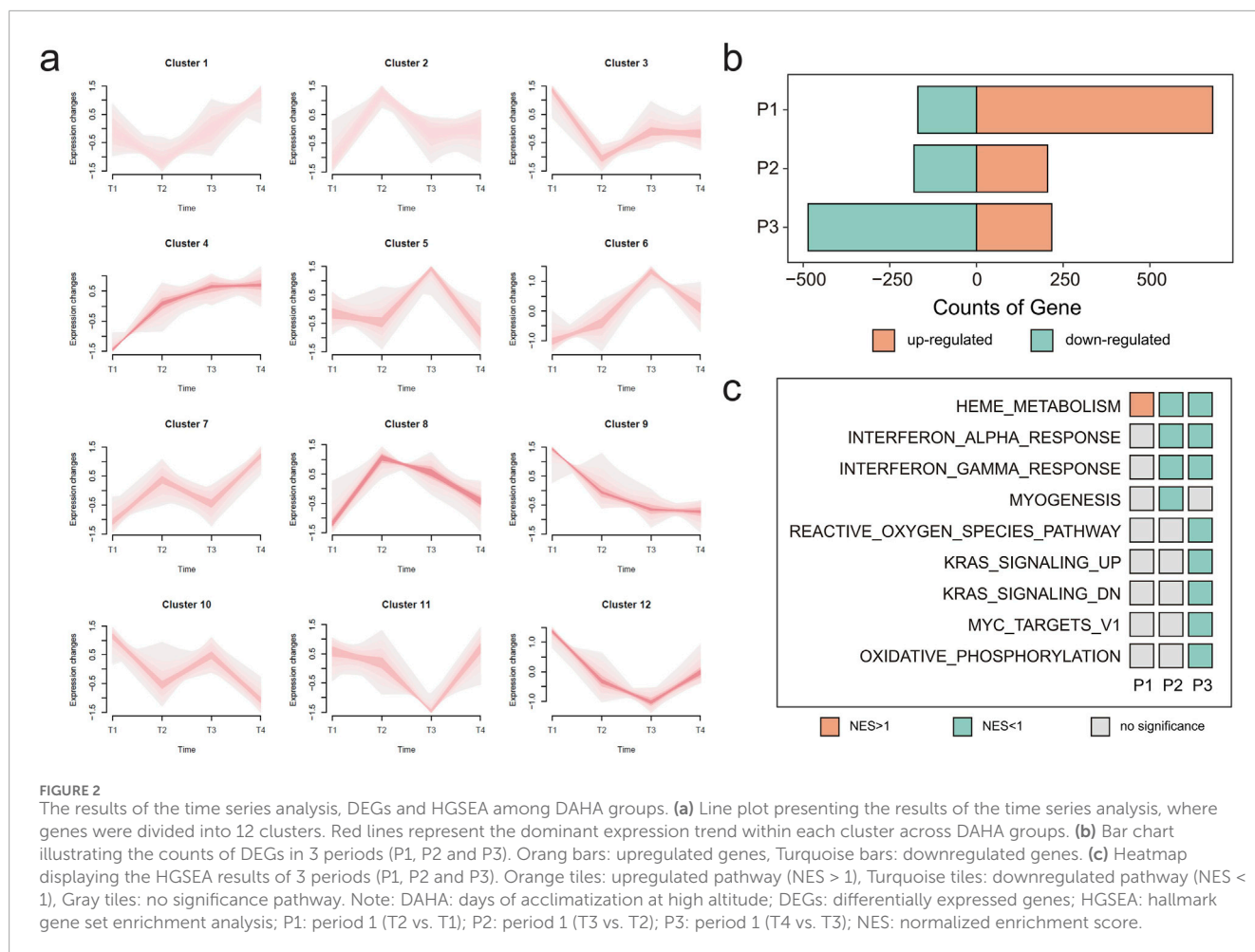
WGCNA revealed distinct gene network expression in DO and BL between the eAMS+ and eAMS- groups (Supplementary Figure S3d). Using a general linear model with AMS experience as the independent variable and DAHA, age, sex and BMI as the covariates, 583 upregulated genes and 104 downregulated genes were identified (Supplementary Table S5). Enrichment analysis showed that the upregulated genes



were involved in adaptive immune response activity, erythrocyte differentiation and the CAMKK2 pathway (Supplementary Figure S7a). Conversely, the downregulated genes were linked to leukocyte-mediated cytotoxicity and antibacterial humoral response (Supplementary Figure S7b).

We identified 398 upregulated genes and 10 pathways shared with Pattern 2, such as gas transport, erythrocyte differentiation, autophagy regulation and so on. In addition, only one downregulated gene overlapped with Pattern 1, though both showed

enrichment in immune response and interferon gamma signaling (Figures 4a,b). The HGSEA results further revealed upregulation of heme metabolism and xenobiotic metabolism pathway, and downregulation of interferon response and inflammatory pathways in the eAMS + group (Figure 4c). Heme metabolism was also found in Pattern 2, while the interferon responses were common in Pattern 1 (Figure 4d). These findings highlight molecular distinctions between eAMS+ and eAMS- groups and their strong association with both Pattern 1 and Pattern 2.



## 2.8 *BCL2L1*, *DCAF12*, *CDC34*, *PINK1*, and *UBB* were identified as potential biomarkers for AMS prediction and the acclimation process

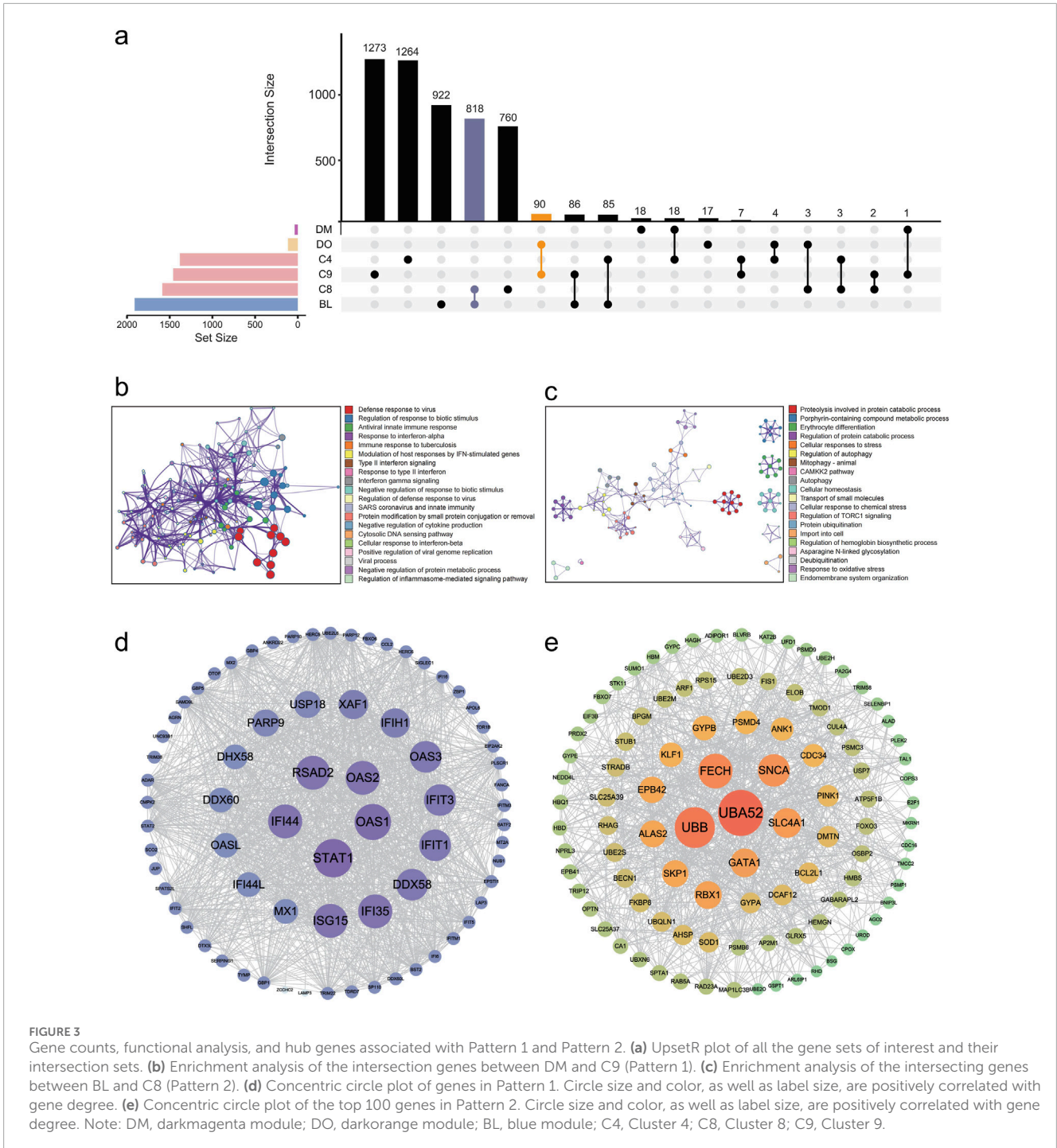
To contextualize our findings, we integrated our Pattern 2 data with the public dataset GSE75665, which tracks transcriptomic changes in human blood before and after 3-day high-altitude exposure. After high-altitude exposure, 679 genes were upregulated and 1,020 downregulated compared with their baseline conditions. Of these, 211 upregulated genes overlapped with Pattern 2 in our study. Enrichment analysis revealed that the gene set shared was primarily associated with proteolysis, erythrocyte differentiation, porphyrin metabolism, and the regulation of autophagy and protein catabolism (Figures 5a,b).

At low altitudes, 64 of the 182 DEGs between AMS and non-AMS groups overlapped with Pattern 2. These included five Pattern 2 hub genes (*BCL2L1*, *DCAF12*, *CDC34*, *PINK1* and *UBB*), highlighting their potential as predictive biomarkers for AMS (Figure 5c). After high-altitude exposure, the overlapped genes with Pattern 2 increased to 128 DEGs with eleven hub genes (*ALAS2*, *BCL2L1*, *DCAF12*, *CDC34*, *EPB42*, *GATA1*, *PINK1*, *PSMD4*, *SNCA*, *UBA52*, and *UBB*) including the five initial biomarkers (Figure 5d). Conversely, in the GSE75665 data, Pattern 1 was nearly absent, found

in none of the 182 low-altitude DEGs and only 2 high-altitude DEGs (*EIF2AK2* and *TRIM22*) (Figure 5c; Supplementary Tables S6,S7).

## 3 Discussion

In our research, the phenotypic responses and molecular expression patterns were examined and analyzed among the Chinese Han individuals following exposure to an altitude of 4,014 m over a period of 23 days. The biological response to prolonged high-altitude exposure is complex and temporally dependent (Figure 2a). SpO<sub>2</sub>, HGB, HCT, and RDW-SD exhibited positive linear relationships with DAHA. Using a combination of transcriptomics analysis and WGCNA, a decreasing expression pattern (Pattern 1) and a “mountain-shaped” expression pattern (Pattern 2) were identified. Pattern 1 was associated with immunity-related pathways, and Pattern 2 was associated with protein ubiquitination and catabolic processes, erythrocyte differentiation, cellular autophagy, and mitophagy. Nearly all the hub genes in Pattern 2 correlated with the physiological parameters, indicating that Pattern 2 could be involved primarily in the process of acclimatization to high altitudes. Compared with those in the eAMS-group, 583 upregulated DEGs and 104 downregulated DEGs were found in the eAMS + group. Among them, 398 upregulated genes



and 10 pathways were associated with Pattern 2, whereas one downregulated gene and two pathways overlapped with Pattern 1, indicating that the molecular differences between the eAMS+ and eAMS- groups were associated with both Pattern 1 and Pattern 2. By integrating low-altitude baseline data from the GSE75665 database, five DEGs before and after altitude exposure that matched the hub genes of Pattern 2 were identified. These findings suggested that the five hub genes could serve as potentially predictive biomarkers for AMS and may be differentially involved in the high-altitude acclimatization process between the eAMS+ and eAMS- groups.

Our study revealed that the SpO<sub>2</sub>, HGB, HCT, and RDW-SD levels gradually increased over time (Figure 1c). The increasing trend of SpO<sub>2</sub> and pulse rate (P) after exposure to high altitude was consistent with the findings of previous studies (Gaur et al., 2020). Milledge and Cotes (1985) observed that serum erythropoietin levels increased one and 2 days after reaching an altitude of 3,500 m and then returned to baseline values even when the elevation increased to 4,500 m. However, the HCT level continued to rise steadily, as evidenced by the gradual increase in HGB and HCT levels in our findings. RDW-SD, which reflects changes in the

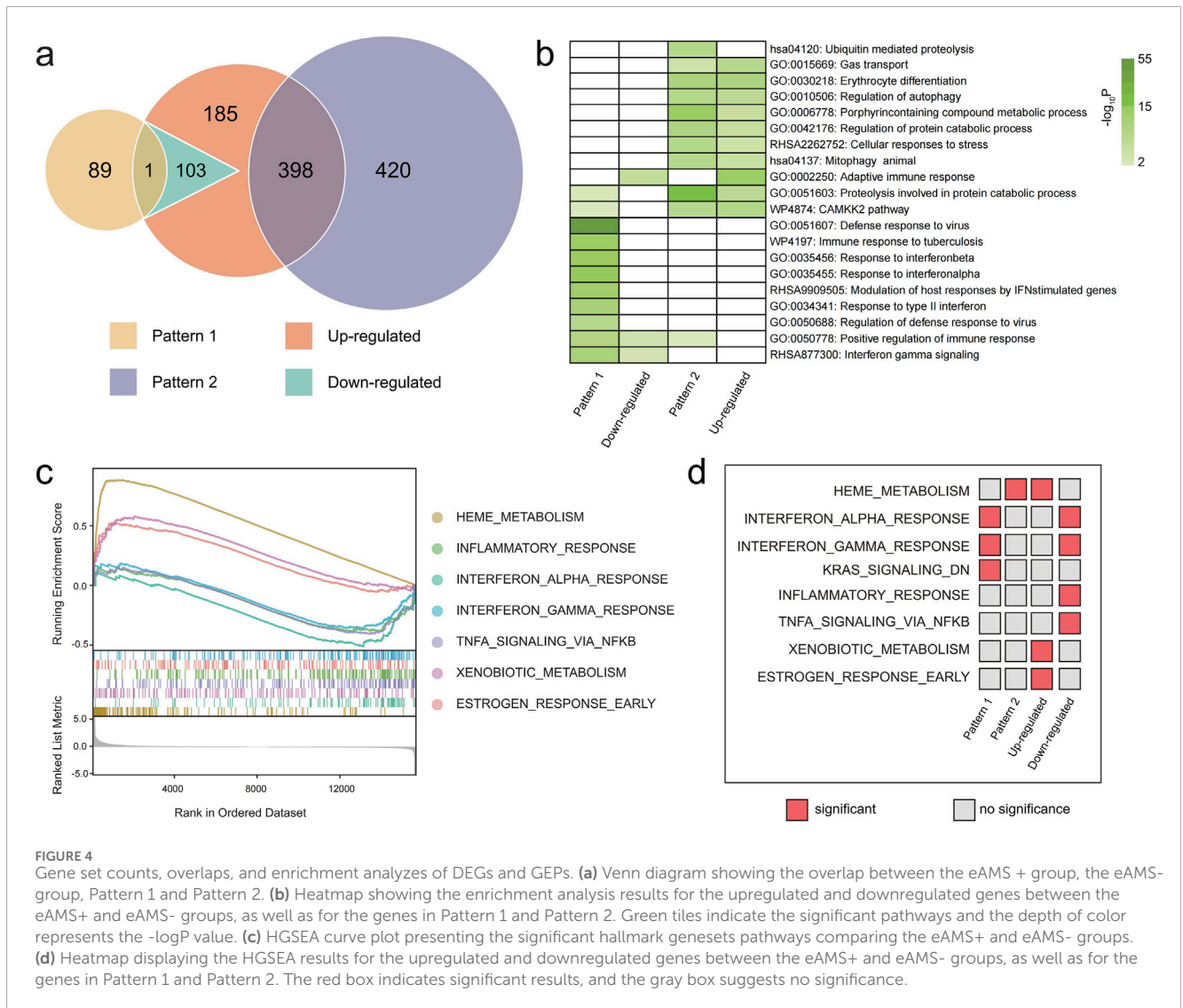


FIGURE 4

Gene set counts, overlaps, and enrichment analyses of DEGs and GEPs. (a) Venn diagram showing the overlap between the eAMS+ group, the eAMS- group, Pattern 1 and Pattern 2. (b) Heatmap showing the enrichment analysis results for the upregulated and downregulated genes between the eAMS+ and eAMS- groups, as well as for the genes in Pattern 1 and Pattern 2. Green tiles indicate the significant pathways and the depth of color represents the  $-\log_{10}P$  value. (c) HGSEA curve plot presenting the significant hallmark genesets pathways comparing the eAMS+ and eAMS- groups. (d) Heatmap displaying the HGSEA results for the upregulated and downregulated genes between the eAMS+ and eAMS- groups, as well as for the genes in Pattern 1 and Pattern 2. The red box indicates significant results, and the gray box suggests no significance.

size of erythrocytes, also gradually increased, altogether suggesting that erythrocytes underwent various degrees of modifications to enhance their oxygen delivery capacity. Almost all the hub genes of Pattern 2 were negatively correlated with HCT, RBC, WBC, and HGB. These findings suggest that the hub genes in Pattern 2 are involved mainly in pathways related to heme metabolism and erythropoiesis. The physiological parameters confirmed this result. The lower the parameters, such as hemoglobin, the higher the gene expression of this pattern. Acute systemic hypoxia and long-term renal hypoperfusion may cause creatinine to increase (Zhou et al., 2013), however, the direct correlation between creatinine and heme metabolism is unclear. These findings suggest that erythrocyte-related indicators accompanied by heme metabolism and erythropoiesis are important hypoxic response to prolonged high-altitude exposure.

Although some studies have explored molecular changes (Yang et al., 2024; Pham et al., 2024) within the first 3 day high-altitude exposure are associated with the pathogenesis of AMS, the patterns of gene expression following prolonged exposure exceeding 3 days are rarely investigated. Previous studies have

shown that upregulated pathways include those involved in blood gas transport, increased erythrocyte development and differentiation, and the heme biosynthetic process during the first 3 day high-altitude exposure (Zhao et al., 2024). Priya Gaur and her colleagues (Gaur et al., 2020) explored physiological parameters and differentially expressed genes at high altitudes on days 3, 7, 14, and 21. In this study, day 3 at high altitude was found to be a distinct time point. However, none of the sea-level volunteers experienced or were experiencing AMS, and the gene expression patterns were not analyzed. In our study, we analyzed the temporal gene expression dynamics of individuals and identified the “mountain-shaped” GEP (Pattern 2) for the first time. This pattern indicated that the peak occurred at T2, which was 3–7 days after ascending to high altitude. This finding suggested that although clinical symptoms visibly alleviate within 7 days, molecular expression remains increasing. The transcripts in Pattern 2 are associated primarily with these pathways, e.g. erythrocyte differentiation, proteolysis, autophagy, mitophagy, gas transport, and CAMKK2, some of which have been mentioned in previous studies (Zhao et al., 2024). These results

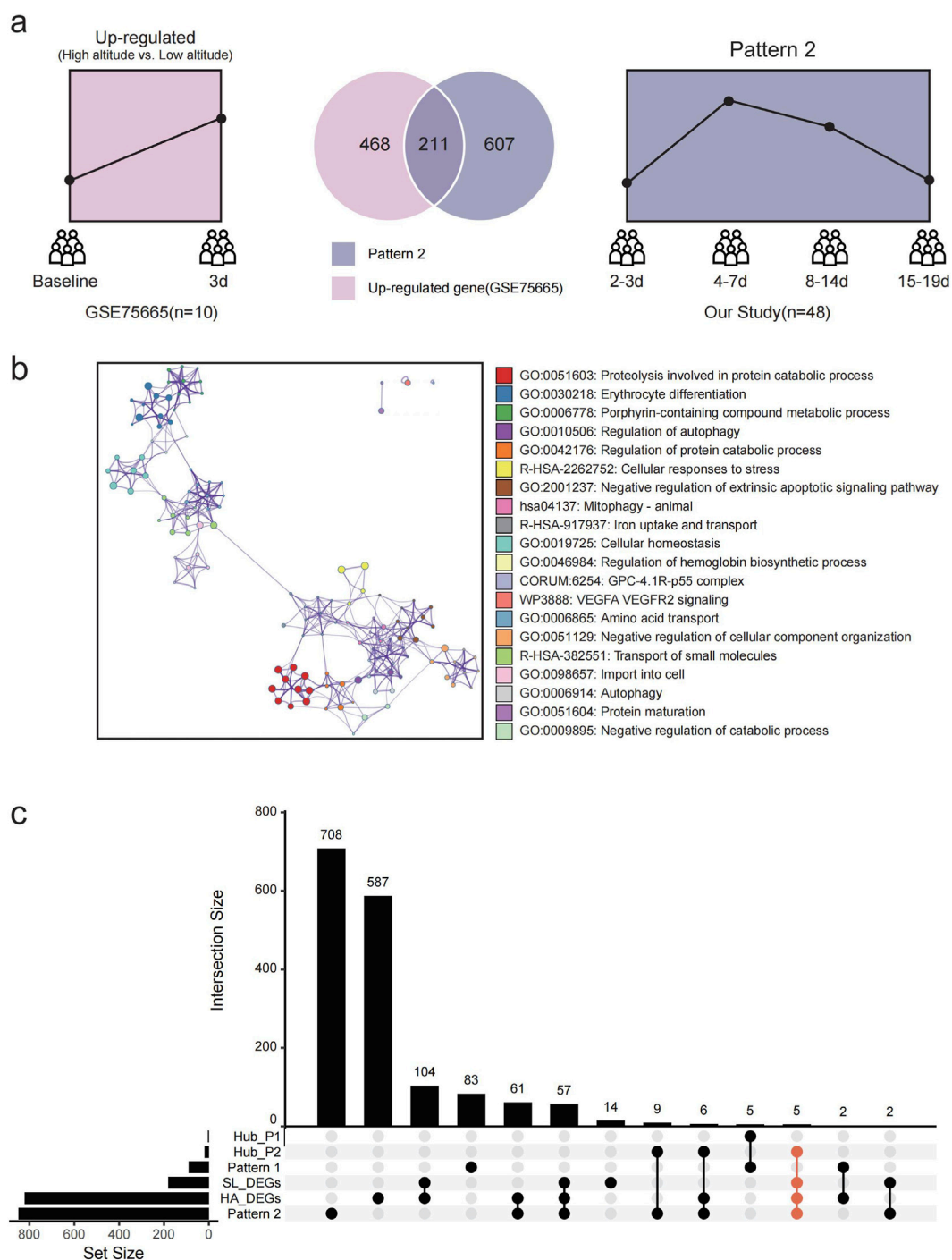


**FIGURE 5** Changes in gene expression from low altitude to high altitude in Pattern 2. **(a)** Trends and counts of upregulated genes in GSE75665 and in Pattern 2 identified in our study. Pink: data from GSE75665, Darkblue: data from our study. **(b)** Enrichment analysis results for the genes shared between the upregulated genes in GSE75665 and Pattern 2 from our study. **(c)** UpSetR plot showing gene sets of Pattern 1, Pattern 2, hub genes in Patterns 1 and 2, DEGs from sea level and high altitude in dataset GSE75665, and their overlaps.

indicated that these biological processes persisted at least until the 7th day after acute ascent to high altitude.

The stability of redox status (Paul et al., 2018), immune and inflammatory responses (Pham et al., 2024; Song et al., 2016), and erythropoiesis (Pham et al., 2024; Tomar et al., 2015) are important

pathways during the acute altitude acclimatization process. It remains unclear what differences in bioinformatics pathways are between individuals with and without AMS. Our study revealed that the eAMS + group presented a transcriptional profile indicative of an enhanced yet potentially dysregulated adaptive response.

Specifically, “enhanced” acclimatization in this context refers to the broad activation of immune and hypoxia-responsive pathways, reflecting an intensified systemic effect to cope with hypoxic stress. In contrast, “dysregulated” acclimatization is suggested by the coexistence of immune activation with impaired downstream effector functions. Although pathways related to adaptive immunity are significantly upregulated in eAMS + individuals, the concurrent downregulation of leukocyte-mediated cytotoxicity and neutrophil degranulation suggests a disconnect immune signaling and effective immune execution. Such an imbalance may result in insufficient pathogen clearance or prolonged, unresolved inflammation, thereby contributing to AMS pathophysiology. Conversely, the increase in erythrocyte differentiation and gas transport represents a canonical compensatory effort to enhance oxygen delivery (Golden et al., 1981) in response to hypoxic stress. However, the significant enrichment of hydrogen peroxide catabolic processes points to elevated oxidative stress (Rojkind et al., 2002), which may exacerbate cellular damage. The increased activity of CAMKK2, a key hypoxia-sensitive pathway (Li C. et al., 2023), further supports a heightened metabolic stress response in eAMS + individuals. These three pathways, including heme metabolism, overlapping with Pattern 2, the interferon alpha response, and the interferon gamma response overlapping with Pattern 1, were more significant in eAMS + individuals than in eAMS- individuals (Figure 4d). These findings indicate that eAMS + individuals experience more pronounced physiological disruption and immune dysregulation. Overall, the eAMS + group presented greater metabolic stress and more significant immune suppression, highlighting key mechanisms underlying its poorer acclimatization to high-altitude environments.

Molecular biomarkers are crucial in high-altitude pathophysiological conditions. One study identified candidate genes controlling cellular interactive pathways suggesting that hypoxia affects the structure and function of endothelial cells (Pham et al., 2024). Another study highlighted ten key genes involved in blood gas transport, erythrocyte development and differentiation, and heme biosynthetic process. Two of these key genes, FECH and ALAS2, play crucial roles in the heme biosynthetic pathway (Norboo et al., 2004), which was also detected in our hub 20 genes of Pattern 2 (Figure 3e). Through joint analysis with the GSE75665 database in our study, five predictive hub genes (*BCL2L1*, *DCAF12*, *CDC34*, *PINK1* and *UBB*) were identified and were significantly differentially expressed between the AMS group and the non-AMS group before and after high altitude exposure. These five hub genes form a synergistic network: *BCL2L1* promotes cellular survival (Chen et al., 2015), *DCAF12* (Jiao et al., 2022; Patron et al., 2019) and *CDC34* (Ben-Neriah, 2002) enable targeted degradation, regulating specific stress responses, inflammation, and the cell cycle; *PINK1* regulates hypoxia-related mitochondrial function, and *UBB* underpins essential proteostasis. The coordinated expression of these genes reflects the cellular struggle to maintain homeostasis under hypoxic stress, making them candidates for a multi-gene AMS prediction panel. These five genes serve as crucial molecules within the intricate biological processes of apoptosis and ubiquitination which play vital roles in the hypoxic environment. *ALAS2*, *BCL2L1* and *DCAF12* have been found to be significantly expressed 10 days after arriving at altitude, and *BCL2L1* had the highest

sensitivity and specificity following application of the adaptive model (Wang et al., 2017). Controlling the mitochondria quality by promoting PINK1/parkin-dependent mitophagy and mitochondrial fission could alleviate AMS (Tian et al., 2023; Li Y. P. et al., 2023). Interestingly, *CDC34* and *UBB* are rarely mentioned in previous hypoxic or high-altitude studies. Further validation through clinical investigations and experimental studies is essential to establish their predictive value. This could ultimately contribute to improved strategies for the prevention and management of AMS in vulnerable Han populations, such as workers and travelers in high-altitude environments (Norboo et al., 2004; Fiore et al., 2010).

## 4 Limitations

Several limitations should be considered when interpreting our findings. Firstly, due to cross-sectional design, physiological and transcriptomic profiles obtained from different individuals at varying DAHA enables the identification of population-level exposure-associated trends, but they do not permit direct inference of within-individual longitudinal dynamics. Accordingly, the two gene expression patterns identified in this study should be interpreted as exposure duration-associated expression profiles across the cohort rather than true dynamic trajectories within the same individual. Additionally, AMS symptoms within the first 3 days after ascent were assessed using a standardized questionnaire, and for some participants were recorded retrospectively based on recall, which may introduce recall bias despite the short recall window. Moreover, owing to the lack of baseline data before exposure to high altitude, this study conducted a comprehensive analysis by integrating the baseline data from the GSE75665 database, which may introduce residual variability.

Finally, while *CDC34* and *UBB* were identified as novel hub genes associated with Pattern 2 and AMS susceptibility, their functional role in high-altitude acclimatization remains to be experimentally validated. Future studies employing hypoxia-treated cell culture models (such as endothelial cells, immune cells, or erythroid progenitors) as well as *in vivo* hypoxia or high-altitude animal models could be used to investigate the mechanistic involvement of *CDC34* and *UBB* mediated pathways in hypoxic acclimatization, inflammatory regulation, and cellular stress responses. Such longitudinal and experimental approaches will be essential to confirm causality and to further elucidate the molecular mechanisms underlying high-altitude acclimatization.

## 5 Conclusion

Our research provides significant insights into the gene expression patterns associated with the process of prolonged high-altitude exposure. Furthermore, physiological and molecular responses were significantly different between individuals with and without eAMS during the acclimatization process. The hub genes were not only potential predictive biomarkers for AMS but also key biomarkers participating in the acclimatization process.

## 6 Research design and methods

### 6.1 Study design

The study was designed as a cross-sectional investigation of physiological and molecular characteristics associated with high-altitude exposure. A total of 113 Chinese Han individuals who recently arrived at a high altitude (LiTang, 4,104 m) were enrolled between February 29th and 6 March 2024. And those with diabetes, respiratory disease, cardiovascular or neurological diseases were excluded. All participants underwent a single standardized physical examination and blood sampling during their stay at high altitude. Meanwhile, participants completed structured case report form (CRF) questionnaires to document demographic characteristics and AMS symptoms occurring within the first 3 days after ascent. Throughout the high-altitude exposure period, they received standardized meals with comparable nutritional contents and were living and working in the same environment. The study was approved by the Ethics Committee of West China Hospital (No. 2021–716). All participants provided written informed consent for the use of their samples and data for research purposes.

### 6.2 Diagnosis of AMS

The symptoms of AMS include headache, gastrointestinal issues, fatigue and/or weakness, and dizziness/light-headedness. AMS was diagnosed via the 2018 Lake Louise Acute Mountain Sickness Score (LLAMS) (Roach et al., 2018), which identifies individuals with a headache score of at least one point and a cumulative score of at least 3 points. For participants who examined within the first 3 days after ascent, AMS symptoms were recorded prospectively. For participants who had already resided at high altitude for more than 3 days at the time of assessment, AMS symptoms occurring within the first 3 days after ascent were recorded retrospectively based on participant recall, using a structured questionnaire administered by trained investigators. Participants who experienced or were experiencing AMS during the early post-ascent period were defined as the eAMS+ group, and individuals who did not meet these criteria were classified as eAMS- group, which served as the internal control group.

### 6.3 Blood collection and storage

Blood was collected from a peripheral vein after 12 h of fasting at high altitude. As this was a cross-sectional study, blood sampling was performed once at a single time point for each individual. The duration of high-altitude exposure at the time of blood collection was retrospectively determined based on each participant's documented arrival date at high altitude, resulting in exposure durations ranging from 1 to 23 days.

Blood samples collected for complete blood cells (CBC) count and blood biochemical tests were immediately sent to LiTang County People's Hospital for testing. A subset of 48 participants, selected from the overall cohort, provided samples for RNA sequencing. All blood samples of the RNA-sequencing set were stored at  $-80^{\circ}\text{C}$  with PAXgene Blood RNA Tubes

(PAXgene, PreAnalytix, Hombrechtikon, Switzerland, distributed by Qiagen, catalog no. 762165) until subsequent RNA extraction and sequencing.

### 6.4 RNA extraction, library construction, sequencing and analysis

Total RNA was extracted from blood samples collected from a subset of 48 participants selected from the original cohort of 113 individuals, using lysis, PAXgene spin columns, and DNase treatment. After quality assessment, mRNA was enriched, globin mRNA removed, and fragmented for cDNA synthesis. Following library preparation with dUTP-based second-strand synthesis, end repair, A-tailing, and adapter ligation, DNA nanoballs (DNBs) were generated and sequenced on the BGI-T7 platform (BGI-Shenzhen, China) using combinatorial probe-anchor synthesis (cPAS) to achieve high-throughput pairwise sequencing.

The raw sequencing data were filtered via SOAPnuke (Chen et al., 2018) (version 1.6.5) to remove the following reads: 1) reads containing adapters (adapter contamination), 2) reads with an unknown base N content exceeding 1%, and 3) low-quality reads (where the proportion of bases with a quality score below 15 exceeded 40% of the total read length). Clean reads were aligned to the *Homo sapiens* reference genome (GRCh38.p14) via STAR (Dobin et al., 2013) (version 2.7.10b) and gene expression counts were quantified via featureCounts (Liao et al., 2014) (version 2.0.4). Normalization was calculated via the trimmed mean of M values (TMM) method in the R package edgeR (Robinson et al., 2010) (version 4.0.16). Differentially expressed genes (DEGs) between the eAMS+ and eAMS- groups were identified using Generalized Linear Model (GLM) (adjusted for DAHA, age, sex and BMI) with significance defined as  $p < 0.05$  and  $|\log_{2}\text{FC}| > 0.3785$ .

### 6.5 Time series expression analysis and coexpression network analysis

Based on the duration of high-altitude acclimatization (Lucas et al., 2011; Gaur et al., 2020), the subset of 48 participants for RNA sequencing analysis had exposure duration ranging from 2 to 19 days (Supplementary Figure S2a). These participants were divided into 4 time-point groups (T1:  $\leq 3$  days; T2: 4–7 days; T3: 8–14 days; T4: 15–19 days) (Supplementary Figure S2b). Time series gene expression analysis was performed using FCM algorithm from the R package Mfuzz (Kumar and E Futschik, 2007) (version 2.62.0) to categorize genes into 12 clusters on the 4 time-point groups. Furthermore, Weighted Co-Expression networks were constructed using the R package WGCNA (Langfelder and Horvath, 2008) (version 1.73) to identify the relationships among genes and investigate their associations with specific traits.

### 6.6 Enrichment and protein-protein interaction analysis

Gene enrichment analysis was conducted via the Metascape (Zhou et al., 2019) (version 3.5) (<https://metascape.org/>) with

default settings by inputting unique gene symbols from each gene set of interest. Hallmark Gene Set Enrichment Analysis (GSEA) (Subramanian et al., 2005) was utilized to identify significant pathways ( $p < 0.05$ ,  $q < 0.25$ ,  $|NES| > 1$ ) between the AMS and non-AMS groups. PPI network from STRING (Szklarczyk et al., 2023) (version 12.0) (<https://string-db.org/>) was visualized in Cytoscape (Shannon et al., 2003) (version 3.10.3). Hub genes were defined as those in the top 2.5% or 5% of node degree based on the size of the gene set.

## 6.7 Public data collection and analysis

For compensating the lack of baseline data and prediction biomarker identification, we conducted a systematic literature search for studies associated with AMS. Inclusion criteria were: 1). The transcriptomics data is available; 2). The participants should have baseline data and AMS outcomes following high-altitude exposure; 3). As genetic and environmental heterogeneity significantly influences gene expression patterns (Martin et al., 2014), we restricted the baseline data to the Chinese population. Following our inclusion criteria, only one public transcriptome data GSE75665 (Liu et al., 2017) was included. This dataset comprised 20 samples divided into two groups (AMS and non-AMS) and two time points (baseline and 72 h after high-altitude exposure). DEGs based on longitudinal groups were analyzed via a density-based pruning algorithm. For the baseline cross-sectional comparison (AMS vs. non-AMS = 5 vs. 5), we employed the same analytical approach, excluding the lowest 10% expressed genes and considering  $|\log_{2}FC| > 0.3785$  as statistically significant.

## Data availability statement

The data presented in this study are deposited in the China National Center for Bioinformatics (CNCB-NGDC) repository, accession number OMIX011838.

## Ethics statement

The studies involving humans were approved by Ethics Committee of West China Hospital. The studies were conducted in accordance with the local legislation and institutional requirements. The participants provided their written informed consent to participate in this study.

## Author contributions

LiC: Funding acquisition, Resources, Writing – review and editing, Writing – original draft, Data curation, Visualization, Methodology, Project administration, Conceptualization. XH: Writing – review and editing, Software, Supervision, Visualization, Writing – original draft, Data curation. HW: Methodology, Project administration, Supervision, Data curation, Writing – review

and editing, Investigation. SH: Software, Writing – original draft, Visualization, Methodology. HZ: Data curation, Methodology, Writing – original draft, Investigation. GN: Writing – original draft, Data curation, Methodology, Investigation. HY: Resources, Writing – review and editing, Data curation, Supervision, Methodology. LeC: Conceptualization, Methodology, Data curation, Investigation, Writing – review and editing, Funding acquisition. CD: Methodology, Project administration, Supervision, Funding acquisition, Formal Analysis, Writing – review and editing. FL: Supervision, Conceptualization, Methodology, Project administration, Investigation, Writing – review and editing, Resources, Data curation.

## Funding

The author(s) declared that financial support was received for this work and/or its publication. This study was supported by Post-Doctor Research Project (2024HXBH035, 2024HXBH060), 1.3.5 Project of Center for High Altitude Medicine (GYYX24001), Scientific and Technological Innovation 2030-Major Project (2023ZD0505300, 2023ZD0505306), and National Natural Science Foundation of China (32270438).

## Acknowledgements

We are grateful to all the participants in this study. We would like to thank colleagues from West China Biobank, West China Hospital, Sichuan University for their invaluable assistance with biospecimen collection, processing, quality control, and storage.

## Conflict of interest

The author(s) declared that this work was conducted in the absence of any commercial or financial relationships that could be construed as a potential conflict of interest.

## Generative AI statement

The author(s) declared that generative AI was not used in the creation of this manuscript.

Any alternative text (alt text) provided alongside figures in this article has been generated by Frontiers with the support of artificial intelligence and reasonable efforts have been made to ensure accuracy, including review by the authors wherever possible. If you identify any issues, please contact us.

## Publisher's note

All claims expressed in this article are solely those of the authors and do not necessarily represent those of

their affiliated organizations, or those of the publisher, the editors and the reviewers. Any product that may be evaluated in this article, or claim that may be made by its manufacturer, is not guaranteed or endorsed by the publisher.

## References

- Basnyat, B., and Starling, J. M. (2015). Infectious diseases at high altitude. *Microbiol. Spectr.* 3 (4). doi:10.1128/microbiolspec.IOL5-0006-2015
- Ben-Neriah, Y. (2002). Regulatory functions of ubiquitination in the immune system. *Nat. Immunol.* 3 (1), 20–26. doi:10.1038/ni0102-20
- Buroker, N. E., Ning, X.-H., Zhou, Z.-N., Li, K., Cen, W.-J., Wu, X.-F., et al. (2012). EPAS1 and EGLN1 associations with high altitude sickness in Han and Tibetan Chinese at the Qinghai-Tibetan Plateau. *Blood Cells Mol. And Dis.* 49 (2), 67–73. doi:10.1016/j.bcmd.2012.04.004
- Calbet, J. A. L., Rådegran, G., Boushel, R., Søndergaard, H., Saltin, B., and Wagner, P. D. (2002). Effect of blood haemoglobin concentration on V(O<sub>2</sub>,max) and cardiovascular function in lowlanders acclimatized to 5260 m. *J. Physiol.* 545 (2), 715–728. doi:10.1113/jphysiol.2002.029108
- Chen, F., Zhang, W., Fau - Liang, Y., Liang, Y., Fau - Huang, J., Huang, J., et al. (2012). Transcriptome and network changes in climbers at extreme altitudes. 1932–6203.
- Chen, M., Wang, M., Xu, S., Guo, X., and Jiang, J. (2015). Upregulation of miR-181c contributes to chemoresistance in pancreatic cancer by inactivating the Hippo signaling pathway. *Oncotarget* 6 (42), 44466–44479. doi:10.18632/oncotarget.6298
- Chen, Y., Chen, Y., Shi, C., Huang, Z., Zhang, Y., Li, S., et al. (2018). SOAPnuke: a MapReduce acceleration-supported software for integrated quality control and preprocessing of high-throughput sequencing data. *Gigascience* 7 (1), 1–6. doi:10.1093/gigascience/gix120
- Cheng, F., Shen, R.-J., Zheng, Z., Chen, Z. J., Huang, P.-J., Feng, Z.-K., et al. (2025). Distinct methylomic signatures of high-altitude acclimatization and adaptation in the Tibetan Plateau. *Cell. Discov.* 11 (1), 45. doi:10.1038/s41421-025-00795-z
- Dehnert, C., Grünig, E., Meredes, D., von Lennepe, N., and Bärtsch, P. (2005). Identification of individuals susceptible to high-altitude pulmonary oedema at low altitude. *Eur. Respir. J.* 25 (3), 545–551. doi:10.1183/09031936.05.00070404
- Dobin, A., Davis, C. A., Schlesinger, F., Drenkow, J., Zaleski, C., Jha, S., et al. (2013). STAR: ultrafast universal RNA-seq aligner. *Bioinformatics* 29 (1), 15–21. doi:10.1093/bioinformatics/bts635
- Fiore, D. C., Hall, S., and Shoja, P. (2010). Altitude illness: risk factors, prevention, progression, and treatment. *Am. Fam. Physician* 82 (9), 1103–1110.
- Golden, D. W., Hocking, W. G., Koeffler, H. P., and Adamson, J. W. (1981). Polycythemia: mechanisms and management. *Ann. Intern. Med.* 95, 71–87. doi:10.7326/0003-4819-95-1-71
- Gaur, P., Saini, S., Ray, K., Asanbekovna, K. N., Akunov, A., Maripov, A., et al. (2020). Temporal transcriptome analysis suggest modulation of multiple pathways and gene network involved in cell-cell interaction during early phase of high altitude exposure. *PLoS One* 15 (9), e0238117. doi:10.1371/journal.pone.0238117
- Hultgren, H. N. (1979). High altitude medical problems. *West J. Med.* 131 (1), 8–23.
- Jiao, D., Chen, Y., Wang, Y., Sun, H., Shi, Q., Zhang, L., et al. (2022). DCAF12 promotes apoptosis and inhibits NF-κB activation by acting as an endogenous antagonist of IAPs. *Oncogene* 41 (21), 3000–3010. doi:10.1038/s41388-022-02319-5
- Julian, R. J. (2007). The response of the heart and pulmonary arteries to hypoxia, pressure, and volume. A short review. *Poult. Sci.* 86 (5), 1006–1011. doi:10.1093/ps/86.5.1006
- Kohane, I. S., and Valtchinov, V. I. (2012). Quantifying the white blood cell transcriptome as an accessible window to the multiorgan transcriptome. *Bioinformatics* 28 (4), 538–545. doi:10.1093/bioinformatics/btr713
- Kumar, L., and E Futschik, M. (2007). Mfuzz: a software package for soft clustering of microarray data. *Bioinformatics* 2 (1), 5–7. doi:10.6026/97320630002005
- Langfelder, P., and Horvath, S. (2008). WGCNA: an R package for weighted correlation network analysis. *BMC Bioinforma.* 9, 559. doi:10.1186/1471-2105-9-559
- Li, C., Hao, J., Qiu, H., and Xin, H. (2023). CaMKK2 alleviates myocardial ischemia/reperfusion injury by inhibiting oxidative stress and inflammation via the action on the AMPK-AKT-GSK-3β/Nrf2 signaling cascade. *Inflamm. Res.* 72, 1409–1425. doi:10.1007/s00011-023-01756-6
- Li, Y. P., Li, M. X., Wang, C., Li, Y. D., Sa, Y. P., and Guo, Y. (2023). Bloodletting acupuncture at jing-well points on hand induced autophagy to alleviate brain injury in acute altitude hypoxic rats by activating PINK1/Parkin pathway. *Chin. J. Of Integr. Med.* 29 (10), 932–940. doi:10.1007/s11655-023-3597-0
- Liao, Y., Smyth, G. K., and Shi, W. (2014). featureCounts: an efficient general purpose program for assigning sequence reads to genomic features. *Bioinformatics* 30 (7), 923–930. doi:10.1093/bioinformatics/btt656
- Liew, C.-C., Ma, J., Tang, H.-C., Zheng, R., and Dempsey, A. A. (2006). The peripheral blood transcriptome dynamically reflects system wide biology: a potential diagnostic tool. *J. Lab. Clin. Med.* 147 (3), 126–132. doi:10.1016/j.lab.2005.10.005
- Liu, B., Chen, J., Zhang, L., Gao, Y., Cui, J., Zhang, E., et al. (2017). IL-10 dysregulation in acute Mountain sickness revealed by transcriptome analysis. *Front. Immunol.* 8, 628. doi:10.3389/fimmu.2017.00628
- Lucas, S. J. E., Burgess, K. R., Thomas, K. N., Donnelly, J., Peebles, K. C., Lucas, R. A. I., et al. (2011). Alterations in cerebral blood flow and cerebrovascular reactivity during 14 days at 5050 m. *J. Physiol.* 589 (Pt 3), 741–753. doi:10.1113/jphysiol.2010.192534
- Luks, A. M., Swenson, E. R., and Bärtsch, P. (2017). Acute high-altitude sickness. *Eur. Respir. Rev.* 26 (143). doi:10.1183/16000617.0096-2016
- Martin, A. R., Costa, H. A., Lappalainen, T., Henn, B. M., Kidd, J. M., Yee, M. C., et al. (2014). Transcriptome sequencing from diverse human populations reveals differentiated regulatory architecture, 1553–7404.
- Milledge, J. S., and Cotes, P. M. (1985). Serum erythropoietin in humans at high altitude and its relation to plasma renin. *J. Appl. Physiol.* 59 (2), 360–364. doi:10.1152/jappl.1985.59.2.360
- Norboo, T., Saiyed, H. N., Angchuk, P. T., Tsering, P., Angchuk, S. T., Phuntsog, S. T., et al. (2004). Mini review of high altitude health problems in Ladakh. *Biomed. Pharmacother.* 58 (4), 220–225. doi:10.1016/j.biopha.2004.02.003
- Patron, L. A., Nagatomo, K., Eves, D. T., Imad, M., Young, K., Torvund, M., et al. (2019). Cul4 ubiquitin ligase cofactor DCAF12 promotes neurotransmitter release and homeostatic plasticity. *J. Of Cell. Biol.* 218 (3), 993–1010. doi:10.1083/jcb.201805099
- Paul, S., Gangwar, A., Bhargava, K., Khurana, P., and Ahmad, Y. (2018). Diagnosis and prophylaxis for high-altitude acclimatization: adherence to molecular rationale to evade high-altitude illnesses. *Life Sci.* 203, 171–176. doi:10.1016/j.lfs.2018.04.040
- Pham, K., Frost, S., Parikh, K., Puvvula, N., Oeung, B., and Heinrich, E. C. (2022). Inflammatory gene expression during acute high-altitude exposure. *J. Physiol.* 600 (18), 4169–4186. doi:10.1113/JP282772
- Pham, K., Vargas, A., Frost, S., Shah, S., and Heinrich, E. C. (2024). Changes in immune cell populations during acclimatization to high altitude. *Physiol. Rep.* 12 (22), e70024. doi:10.14814/phy2.70024
- Roach, R. C., Hackett, P. H., Oelz, O., Bärtsch, P., Luks, A. M., MacInnis, M. J., et al. (2018). The 2018 Lake Louise acute Mountain sickness score. *High Alt. Med. and Biol.* 19 (1), 4–6. doi:10.1089/ham.2017.0164
- Robinson, M. D., McCarthy, D. J., and Smyth, G. K. (2010). edgeR: a bioconductor package for differential expression analysis of digital gene expression data. *Bioinformatics* 26 (1), 139–140. doi:10.1093/bioinformatics/btp616
- Rojkind, M., Domínguez-Rosales Ja Fau - Nieto, N., Nieto, N., Fau - Greenwel, P., and Greenwel, P. (2002). Role of hydrogen peroxide and oxidative stress in healing responses. *Cell Mol Life Sci.* 59(11):1872–1891. doi:10.1007/pl00012511
- Shannon, P., Markiel, A., Ozier, O., Baliga, N. S., Wang, J. T., Ramage, D., et al. (2003). Cytoscape: a software environment for integrated models of biomolecular interaction networks. *Genome Res.* 13 (11), 2498–2504. doi:10.1101/gr.1239303
- Sharma, V., Varshney, R., and Sethy, N. K. (2022). Human adaptation to high altitude: a review of convergence between genomic and proteomic signatures. *Hum. Genomics* 16 (1), 21. doi:10.1186/s40246-022-00395-y
- Sikri, G., and Bhattachar, S. (2017). Acute mountain sickness amongst tourists to Lhasa. *Arch. Public Health* 75, 4. doi:10.1186/s13690-016-0172-6
- Song, T. T., Bi, Y. H., Gao, Y.-Q., Huang, R., Hao, K., Xu, G., et al. (2016). Systemic pro-inflammatory response facilitates the development of cerebral edema during short hypoxia. *J. Neuroinflammation* 13 (1), 63. doi:10.1186/s12974-016-0528-4
- Subramanian, A., Tamayo, P., Mootha, V. K., Mukherjee, S., Ebert, B. L., Gillette, M. A., et al. (2005). Gene set enrichment analysis: a knowledge-based approach for interpreting genome-wide expression profiles. *Proc. Natl. Acad. Sci. U. S. A.* 102 (43), 15545–15550. doi:10.1073/pnas.0506580102
- Subudhi, A. W., Bourdillon, N., Bucher, J., Davis, C., Elliott, J. E., Eutermoster, M., et al. (2014). AltitudeOmics: the integrative physiology of human acclimatization

## Supplementary material

The Supplementary Material for this article can be found online at: <https://www.frontiersin.org/articles/10.3389/fphys.2026.1763837/full#supplementary-material>

- to hypobaric hypoxia and its retention upon reascent. *PLoS One* 9 (3), e92191. doi:10.1371/journal.pone.0092191
- Swenson, E. R. (2013). Hypoxic pulmonary vasoconstriction. *High Alt. Med. and Biol.* 14 (2), 101–110. doi:10.1089/ham.2013.1010
- Swenson, E. R., Duncan, T. B., Goldberg, S. V., Ramirez, G., Ahmad, S., and Schoene, R. B. (1985). Diuretic effect of acute hypoxia in humans: relationship to hypoxic ventilatory responsiveness and renal hormones. *J. Appl. Physiol.* 78 (2), 377–383. doi:10.1152/jappl.1995.78.2.377
- Szklarczyk, D., Kirsch, R., Koutrouli, M., Nastou, K., Mehryary, F., Hachilif, R., et al. (2023). The STRING database in 2023: protein-protein association networks and functional enrichment analyses for any sequenced genome of interest. *Nucleic Acids Res.* 51 (D1), D638–D646. doi:10.1093/nar/gkac1000
- Tian, L., Jia, Z., Yan, Y., Jia, Q., Shi, W., Cui, S., et al. (2023). Low-dose of caffeine alleviates high altitude pulmonary edema *via* regulating mitochondrial quality control process in AT1 cells. *Front. Pharmacol.* 14, 1155414. doi:10.3389/fphar.2023.1155414
- Tomar, A., Malhotra, S., and Sarkar, S. (2015). Polymorphism profiling of nine high altitude relevant candidate gene loci in acclimatized sojourners and adapted natives. *BMC Genet.* 16, 112. doi:10.1186/s12863-015-0268-y
- Wang, G., Durussel, J., Shurlock, J., Moores, M., Fuku, N., Bruinvels, G., et al. (2017). Validation of whole-blood transcriptome signature during microdose recombinant human erythropoietin (rHuEpo) administration. *BMC Genomics* 18 (Suppl. 8), 817. doi:10.1186/s12864-017-4191-7
- Weil, J. V., Byrne-Quinn, E., Sodal, I. E., Friesen, W. O., Underhill, B., Filley, G. F., et al. (1970). Hypoxic ventilatory drive in normal man. *J. Clin. Invest.* 49 (6), 1061–1072. doi:10.1172/JCI106322
- Yang, R., Gautam, A., Hammamieh, R., Roach, R. C., and Beidleman, B. A. (2024). Transcriptomic signatures of severe acute mountain sickness during rapid ascent to 4,300 m. *Front. Physiol.* 15, 1477070. doi:10.3389/fphys.2024.1477070
- Zhang, D., She, J., Zhang, Z., and Yu, M. (2014). Effects of acute hypoxia on heart rate variability, sample entropy and cardiorespiratory phase synchronization. *Biomed. Eng. Online* 13, 73. doi:10.1186/1475-925X-13-73
- Zhao, Y., Zhu, L., Shi, D., Gao, J., and Fan, M. (2024). Key genes FECH and ALAS2 under acute high-altitude exposure: a gene expression and network analysis based on expression profile data. *Genes (Basel)* 15 (8), 1075. doi:10.3390/genes15081075
- Zhou, Y., Zhu, J., and Lin, F. (2013). Acute kidney injury at high altitude. *High Alt. Med. and Biol.* 14 (2), 183–185. doi:10.1089/ham.2012.1123
- Zhou, Y., Zhou, B., Pache, L., Chang, M., Khodabakhshi, A. H., Tanaseichuk, O., et al. (2019). Metascape provides a biologist-oriented resource for the analysis of systems-level datasets. *Nat. Commun.* 10 (1), 1523. doi:10.1038/s41467-019-09234-6

## Glossary

<b>DAHA</b>	duration of acclimatization at high altitude	<b>MCV</b>	mean corpuscular volume
<b>eAMS</b>	the experienced or experiencing acute mountain sickness	<b>MCH</b>	mean corpuscular hemoglobin
<b>AMS</b>	acute mountain sickness	<b>PLT</b>	platelet
<b>HGSEA</b>	hallmark gene set enrichment analysis	<b>RDW-CV</b>	the coefficient of variation of erythrocyte distribution width
<b>WGCNA</b>	weighted gene coexpression network analysis	<b>RDW-SD</b>	the standard deviation of red blood cell distribution width
<b>GEP</b>	gene expression pattern	<b>PCT</b>	plateletcrit
<b>DEGs</b>	differentially expressed genes	<b>PDW</b>	platelet distribution width
<b>FCM</b>	Fuzzy C-Means	<b>MPV</b>	mean platelet volume
<b>CRF</b>	case report form	<b>LYMPH</b>	lymphocyte count
<b>NES</b>	normalized enrichment score	<b>NEUT</b>	neutrophil count
<b> NES </b>	absolute normalized enrichment score	<b>MONOP</b>	the percentage of monocytes
<b> logFC </b>	absolute log fold change	<b>MONO</b>	monocyte count
<b>PPI</b>	protein-protein interaction	<b>BASO</b>	basophils count
<b>PCA</b>	principal component analysis	<b>BASOP</b>	the percentage of basophils
<b>BMI</b>	body mass index	<b>EO</b>	eosinophils count
<b>P</b>	pulse rate	<b>EOP</b>	the percentage of eosinophils
<b>SpO2</b>	saturation of peripheral oxygen		
<b>SBP</b>	systolic blood pressure		
<b>DBP</b>	diastolic blood pressure		
<b>TBIL</b>	total bilirubin		
<b>DBIL</b>	direct bilirubin		
<b>IBIL</b>	indirect bilirubin		
<b>TP</b>	total protein		
<b>ALB</b>	albumin		
<b>GLB</b>	globulin		
<b>AST</b>	aspartate aminotransferase		
<b>ALT</b>	alanine aminotransferase		
<b>CREA</b>	creatinine		
<b>UA</b>	uric acid		
<b>BUN</b>	blood urea nitrogen		
<b>TG</b>	triglyceride		
<b>TC</b>	total cholesterol		
<b>HDLC</b>	high-density lipoprotein cholesterol		
<b>LDLC</b>	low-density lipoprotein cholesterol		
<b>GLU</b>	glucose		
<b>LYMPHP</b>	percentage of lymphocytes		
<b>NEUTP</b>	percentage of neutrophils		
<b>MCHC</b>	mean corpuscular hemoglobin concentration		
<b>HGB</b>	hemoglobin		
<b>RBC</b>	red blood cell count		
<b>HCT</b>	hematocrit		
<b>WBC</b>	white blood cell count		